Delta University Scientific Journal
Journal home page: https://dusj.journals.ekb.eg

Strengthening of seismically deficient moment-resisting frames with yielding metallic dampers

Ahmed Elgammal[1], Yasmin Ali[1], Ayman Seleemah[2]

[1]*Civil Engineering Department, Faculty of Engineering, Delta University for Science and Technology, Gamasa, 11152, Egypt*
[2]*Structural Engineering Department, Faculty of Engineering, Tanta University, Tanta, 31527, Egypt*

Correspondence: Ahmed Elgammal; Gamasa 1152, Egypt; Tel: +20502770140; Fax: +20502770140; Email: ahmed.elgammal@deltauniv.edu.eg

ABSTRACT
Due to the continuous development of codes of practice and design guidelines, existing moment-resisting frames might become deficient because of not satisfying the requirements of them. On the other hand, yielding metallic dampers are one of the most commonly known methods to strengthen deficient buildings to safely withstand seismic excitations. Therefore, this research presents an assessment of the seismic performance of moment-resisting frames strengthened with a particular type of yielding metallic dampers known as the "vertical shear link" using the finite element software ETABS (18.0.0). For this purpose, five-, ten-, and fifteen-story steel buildings that are designed to resist gravity loads only are installed with vertical shear links and their response is evaluated using modal, pushover, and time-history analyses. The vertical shear links are made of either steel or magnesium and they are installed in different locations throughout the buildings. Modal analysis results indicate that the installation of vertical shear links shortens the fundamental period of the buildings. Moreover, the pushover curves underscore the efficiency of vertical shear links in upgrading the performance level of the buildings. However, this does not apply for the fifteen-story building since the number of the installed vertical shear links is found to be not sufficient. Time-history analysis also confirms the same findings since, in contrast to the five- and ten-story buildings, the story displacements and interstory drifts of the fifteen-story building are not significantly decreased after strengthening. Also, the vertical shear links are found to participate in dissipating a considerable amount of seismic energy.

Keywords: *Strengthening; Retrofitting; Eccentrically braced frame; Shear link; Pushover analysis; Time-history analysis.*

1. Introduction

Several existing moment-resisting framed buildings have been designed under the effect of gravity loads only without paying attention to seismic loads. The lack of earthquake-resisting systems in these buildings results in large story displacements and interstory drifts during seismic action. This, in turn, causes significant damage to be applied to the main structural elements of the buildings. For instance, the welded beam-column joints in moment-resisting frames usually exhibit brittle failure at fused zone or column flange zone during the early inelastic action (Lignos et al., 2010). In the same vein, around twenty-three hospitals suspended some or all their services subsequent to the 1994 Northridge earthquake because of the severe cracks they underwent during the seismic excitation. Consequently, the deficient moment-resisting frames should be either modified or strengthened in order to overcome this issue (Shu et al., 2020). Numerous strengthening techniques have been proposed in literature to upgrade the performance of deficient moment-resisting frames (De Matteis & Mistakidis, 2018; TahamouliRoudsari et al., 2018; Tafsirojjaman et al., 2019; Rajeswaran, & Wijeyewickrema, 2022). Among all of them, installation of eccentric braces and yielding metallic dampers is considered as one of the most effective techniques to improve the seismic performance of moment-resisting frames (Di Sarno & Elnashai, 2009; Mazzolani et al., 2009). This is attributed to the fact that eccentrically braced frames combine the advantages of both moment-resisting frames and concentrically raced frames in terms of stiffness and ductility. Although everal devices fall under the category of yielding metallic dampers, shear links represent an example for the most widely used ones.

Conventionally, eccentrically braced frames are equipped with links as shown in Fig. 1. However, replacement of the horizontal links after a severe earthquake were proved to be complex (Mohsenian et al., 2021). Accordingly, several researchers proposed the adoption of replaceable links to enhance the overall performance of the eccentrically braced frame (Mansour et al., 2011; Chesoan et al., 2018; Bozkurt & Topkaya, 2018). Additionally, the adopted links are not necessarily placed horizontally, but they may be placed vertically (Fig. 1). In fact, the process of replacing vertical links is simpler than that of horizontal links (Elgammal, 2021). This configuration of eccentrically braced frames with vertical links was first developed by Seki et al. (Seki et al., 1988) and it has been proved to provide the structure with high stiffness, strength, and ductility. Moreover, this system guarantees stable hysteretic behavior and considerable energy dissipation (Baradaran et al., 2015; Bouwkamp et al., 2016; Vetr et al., 2017). The work of (Zahrai & Mahroozadeh, 2010; Mohsenian & Mortezaei, 2019) illustrated that, in properly designed eccentrically braced frames, the inelastic action is concentrated in the vertical link only. Thus, it acts as a structural fuse that absorbs the earthquake input energy to protect the main structural elements from damage. Therefore, the yield of the vertical link could have shear basis or flexure basis. However, (Duan & Su, 2017) indicated that eccentrically braced frames equipped with vertical shear links have higher ductility and energy dissipation capacity than those with flexure links. (Mohsenian et al., 2020) as well, found out the same observation.

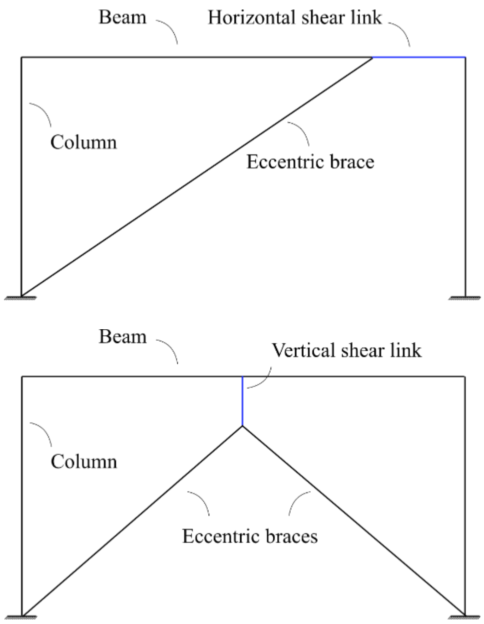

Fig. 1. Typical eccentrically braced frame.

The links are not necessarily made of steel. For instance, (Daryan et al., 2008) investigated easy-going steel vertical shear links. Aluminum vertical shear links were also extensively studied by (Rai et al., 2013). Also, in the numerical work of (EL-Khoriby et al., 2019, 2020), a comparison was made between vertical shear links fabricated from different metallic alloys such as stainless-steel and magnesium. Stainless-steel shear links, in particular, were also tested by (DiSarno et al., 2018; Chacón et al., 2019). In addition, (Ghadami et al., 2021; Zhu et al., 2023) investigated links made of low-yield-point steel, whereas (Mirzai & Attarnejad, 2020) studied shear links made of shape memory alloys.

(El-Gammal et al., 2021; Seleemah et al., 2022) showed that vertical shear links made of different metallic alloys rather than steel can be adopted in different configurations to upgrade the performance of eccentrically braced frames. In the same manner, (Mohsenian, et al., 2020) illustrated that equipping low to medium rise moment-resisting frames with vertical links can improve their overall response. Furthermore, (Rahnavard et al., 2017; Mohsenian & Nikkhoo, 2019) showed that using dual vertical links, in the same panel, instead of one can raise the energy dissipation capacity and the shear carrying capacity. Recently, (Elgammal & Seleemah, 2023) combined horizontal shear links with fluid viscous dampers to enhance the seismic response of steel buildings.

It is seen that the seismic performance of eccentrically braced frames has been widely investigated in literature. In addition, strengthening of moment-resisting frames using eccentric bracing systems have also been addressed and evaluated. Nevertheless, there exists a gap of knowledge in seismic response of multi-story buildings with vertical shear links made of different metallic alloys rather than steel. Hence, this research is considered as an extended study of the work conducted in (El-Gammal et al., 2021; Seleemah et al., 2022) in which magnesium and steel vertical shear links were used in the first few stories of a 10-story building. On this basis, 5, 10, and 15-story 2-D steel moment-resisting frames strengthened using vertical shear links made of magnesium and steel are considered in this research. Each building has six configurations that differ in the fabrication material of the vertical shear link and their characteristics, and the placement location. Firstly, fundamental periods of each configuration were compared to each other. Secondly, a nonlinear static pushover analysis is conducted to show the load-displacement behavior of the configurations and to assess the performance level of each configuration. Thirdly, a nonlinear dynamic time-history analysis is carried out so that the story response plots can be attained and compared. Eventually, hysteretic behavior of the vertical shear links and the hysteretic energy dissipation capacity are, as well, discussed.

2. Description of the buildings

Three 2-D steel moment-resisting framed buildings, having some properties in common, are analyzed in this research when equipped with eccentric braces and vertical shear links. In detail, each of the three buildings consists of three bays of 5 m span for each, and it has a bottom story height of 4.5 m and a typical story height of 3 m. All the beams and columns of the buildings are fabricated from ASTM A572 Gr50 steel which has a tensile yield stress of 345 MPa. Moreover, the foundations of the buildings are assumed to be totally restrained disregarding the effect of soil-structure interaction.
On the other hand, the only differences between the three buildings are the number of stories and the cross-sections of the structural elements. As shown in Fig. 2, the first building (denoted by B5) consists of 5 stories, the second building (denoted by B10) consists of 10 stories and finally, the last building (denoted by B15) consists of 15 stories. Note that the buildings were labeled such that the number of stories could be identified from the label. The buildings were primarily designed, as per (AISC 360, 2016), to resist gravity loads only. The cross-sections of the main structural elements of the buildings are also shown in Fig. 2.

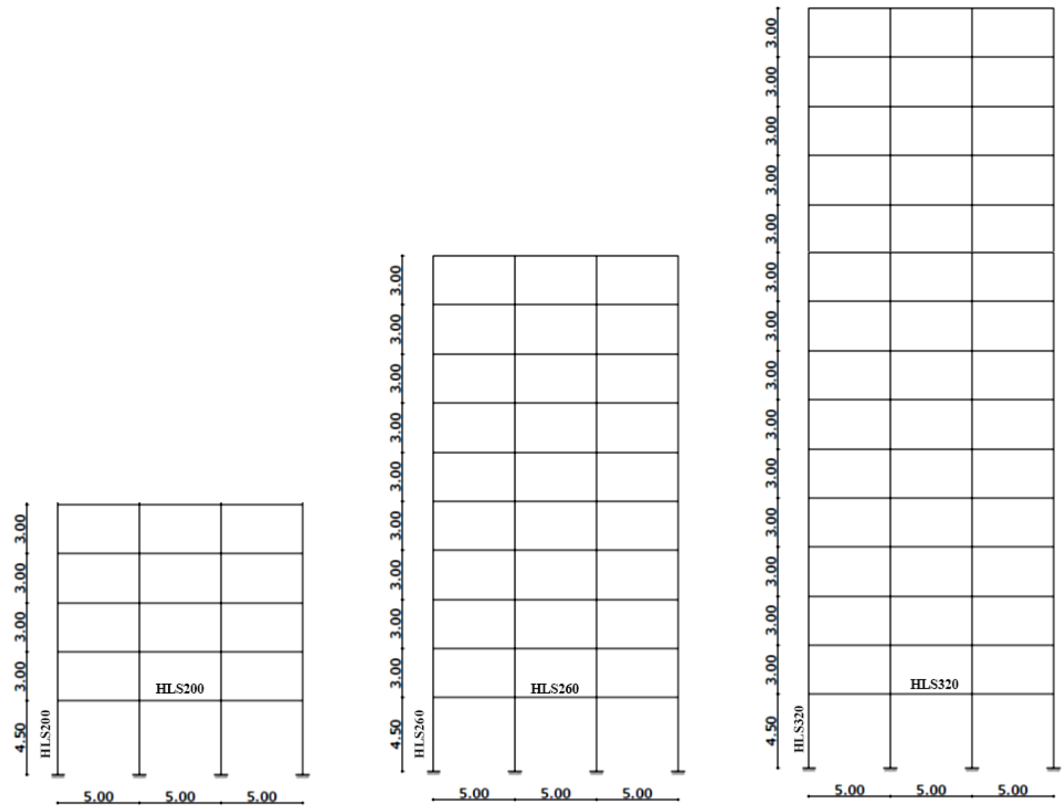

Fig. 2. Elevation view of the buildings.

To strengthen those buildings, their central bays were equipped with vertical shear links along with chevron braces; thereupon, transforming the moment-resisting frames into eccentrically braced frames. To investigate the effect of the fabrication material, the vertical shear links herein were selected to be made of magnesium or steel alloys. Since the current research is an extension of the work in (El-gammal, et al., 2021; Seleemah et al., 2022), the adopted vertical shear links were identical to those in the aforementioned research. Accordingly, Table 1 presents the main mechanical parameters of the four considered vertical shear links, whereas Fig. 3 depicts the skeleton curves extracted from the hysteretic curves of those specimens. For more information related to the hysteretic behavior of those specimens, refer to (El-gammal, et al., 2021; Seleemah et al., 2022).

Table 1. Properties of the shear links reported by (El-gammal, et al., 2021; Seleemah et al., 2022).

Label	Yield shear force (kN)	Elastic stiffness (kN/m)	Post-yield stiffness ratio
Specimen 25	4.32	900	0.125
Specimen 26	10.24	2898	0.148
Specimen 11	12.82	11978	0.073
Specimen 12	30.4	37998	0.026

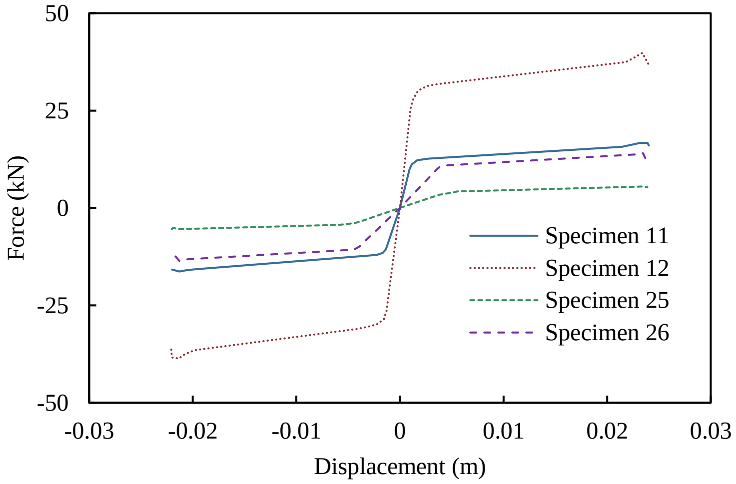

Fig. 3. Skeleton curves of shear force and shear displacement for the vertical shear links

For each building, six different configurations were proposed; one represents the original state of the building without any vertical shear links nor eccentric braces while the other five configurations represent the building installed with vertical shear links in different stories. Accordingly, a total number of eighteen building configurations were studied in the current research. The different configurations proposed for each building are summarized in Table 2. Although it is common, in literature, for vertical shear links to be installed into each story, the vertical shear links in the proposed configurations are only equipped into the first few stories since maximum interstory drifts usually take place at these locations. Therefore, the feasibility of using a limited number of vertical shear links and eccentric braces throughout the building can be investigated. Different configurations oof the buildings are shown in Figs. 5 to 7.

3. Finite element modeling

3.1. Modeling of the main structural elements

In this research, all 18 building configurations were modeled in the commercial finite element software ETABS (18.1.1) (Computers and Structures Inc., 2018). Bases of the buildings were assigned with fixed supports. Beams, columns, and braces were modeled herein using frame elements (Durucan and Dicleli, 2010). To introduce nonlinearity in the FE model, the ends of the beams and columns were assigned with plastic hinges, while the braces were assigned with plastic hinges at their midpoints. The properties of these plastic hinges were determined as per (ASCE/SEI 41, 2017). The assigned plastic hinges for the beams take into account only the bending moment at the major axis of the cross-section (M3). For the columns, the assigned plastic hinges take into account both the bending moment at the major axis (M3) as well as the axial load (P). On the other hand, the plastic hinges of the braces only consider the axial load (P).

Table 2. Locations of the shear links in the building configurations.

Configuration	Story			
	1	2	3	Beyond 3
B5-1	---	---	---	---
B5-2	Specimen 25	---	---	---
B5-3	Specimen 25	Specimen 25	Specimen 25	---
B5-4	Specimen 26	---	---	---
B5-5	Specimen 11	---	---	---
B5-6	Specimen 12	---	---	---
B10-1	---	---	---	---

B10-2	Specimen 25	---	---	---
B10-3	Specimen 25	Specimen 25	Specimen 25	---
B10-4	Specimen 26	---	---	---
B10-5	Specimen 11	---	---	---
B10-6	Specimen 12	---	---	---
B15-1	---	---	---	---
B15-2	Specimen 25	---	---	---
B15-3	Specimen 25	Specimen 25	Specimen 25	---
B15-4	Specimen 26	---	---	---
B15-5	Specimen 11	---	---	---
B15-6	Specimen 12	---	---	---

3.2. Modeling of the vertical shear links

To simulate the hysteretic behavior of vertical shear links when equipped into full-scale structure in ETABS (Computers and Structures Inc., 2018), the vertical shear link should be modelled as a link element assigned with nonlinear properties. The link element is completely defined with stiffness properties rather than section properties. ETABS (Computers and Structures Inc., 2018) includes a wide range of link elements. Nonetheless, Wen plasticity model (Wen, 1976) is the one concerned with vertical shear link modeling in ETABS (Computers and Structures Inc., 2018; Durucan and Dicleli, 2010; Maniyar and Paul, 2012). This plasticity model is based on the hysteretic behavior proposed early by (Wen, 1976). To model vertical shear links using this model, mechanical parameters of the specimens such as yield force, initial stiffness, and post yield stiffness ratio were required. Consequently, the hysteretic characteristics presented, earlier, in Table 1 were used.

3.3. Validation of the finite element model

The FE model created in ETABS (Computers and Structures Inc., 2018) should be validated to ensure ETABS (Computers and Structures Inc., 2018) capability of simulating vertical shear links behavior and capturing eccentrically braced frames response based on the hysteretic data of the vertical shear links. For this purpose, one of the specimens of the experimental tests of (Li et al., 2021) were chosen for this verification study. The specimen was a half-scale 3-D structure representing the top story of a three-story eccentrically braced framed building. Beams and columns were fabricated from Q460 steel with a nominal tensile yield stress of 460 MPa, the braces were fabricated from Q345 steel with a nominal tensile yield stress of 345 MPa. The top story was applied with a monotonic load acting in the same plane containing the eccentrically braced frame in order to perform a nonlinear static pushover analysis. Fig. 4 reveals that the base shear vs. top story displacement curve reported by (Li et al., 2021) is compatible with that of the current finite element model. The ratio of the ultimate base shear from the finite element to the ultimate experimental base shear was 1.15 which is quite acceptable. In the light of this, good agreement was reached, overall, between the finite element analysis results and the experimental results, despite the presence of slight discrepancies. Accordingly, the accuracy of the current numerical solution provides certainty to further study the response of eccentrically braced frames with different characteristics.

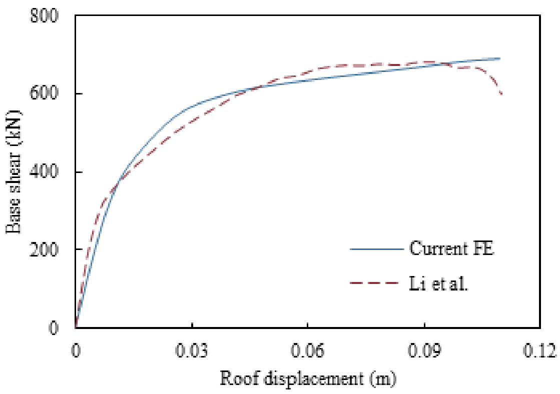

Fig. 4. Comparison between the experimental pushover curve reported by (Li et al., 2021) and the numerical curve of the verification study.

4. Results and evaluation

4.1. Eigenvalue modal analysis

Modal analysis was conducted on the proposed building configurations in order to evaluate the effect of installing vertical shear links on the fundamental period (T). Since the first Eigenvalue mode shape is the dominant in most basic structures, it was the only mode considered in this research.
Fig. 6 depicts the first mode shape of all six configurations of the five-story building (B5) and it is obvious that the overall shape of the first mode is almost identical for each configuration. However, the installation of three vertical shear links in configuration B5-3 restrained the displacements of the second and third story a little bit. It can be also detected from Fig. 5. that installing vertical shear links in the building increased its stiffness which caused a reduction in the fundamental period (T). Yet, the reduction of the fundamental periods for the configurations B5-2 to B5-6 compared to B5-1 ranged from 9 to 31% which is expected to affect the maximum base shear acting on the different configurations, as will be shown later in this section.

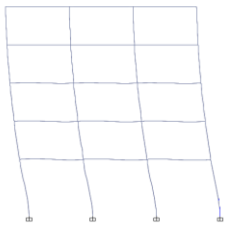

B5-1 ($T = 0.45\ s$)

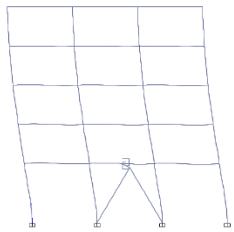

B5-2 ($T = 0.41\ s$)

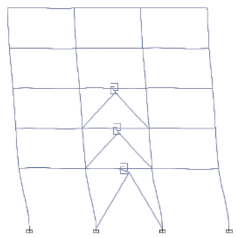

B5-3 ($T = 0.37\ s$)

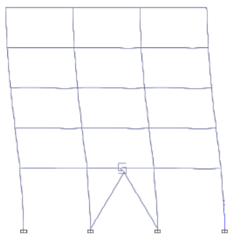

B5-4 ($T = 0.37\ s$)

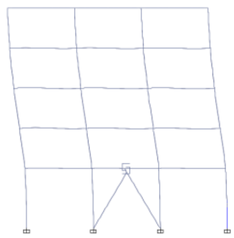

B5-5 ($T = 0.33\ s$)

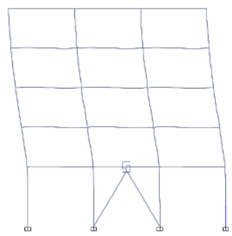

B5-6 ($T = 0.31\ s$)

Fig. 5. First mode shape of the five-story configurations.

Again, the first mode shape of each configuration of the ten-story building (B10), shown in Fig. 6, illustrates that the installation of vertical shear links into the bays of the building did not change the overall first mode shape of each configuration. With regard to the fundamental period (T) of the first mode shape of each configuration, presented in the same figure, it is found that equipping the building with vertical shear links caused the fundamental period (T) of the first mode shape of the configurations to drop by about 3 to 16% compared to the original configuration, which was somehow smaller than the same percentage for the five-story configurations. The reason is that the current ten-story configurations had approximately twice the weight of the five-story configurations. Thus, the installation of the vertical shear links did not have the same significant effect on the fundamental period (T) when compared to the five-story configurations.

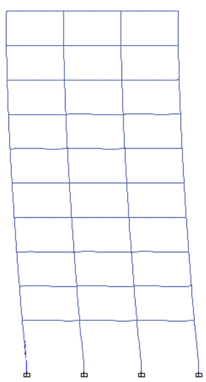

B10-1 ($T = 0.66\ s$)

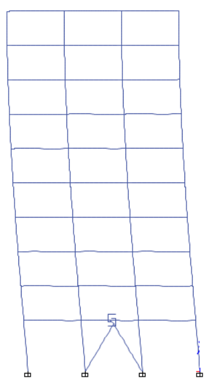

B10-2 ($T = 0.64\ s$)

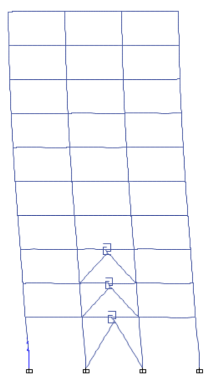

B10-3 ($T = 0.61\ s$)

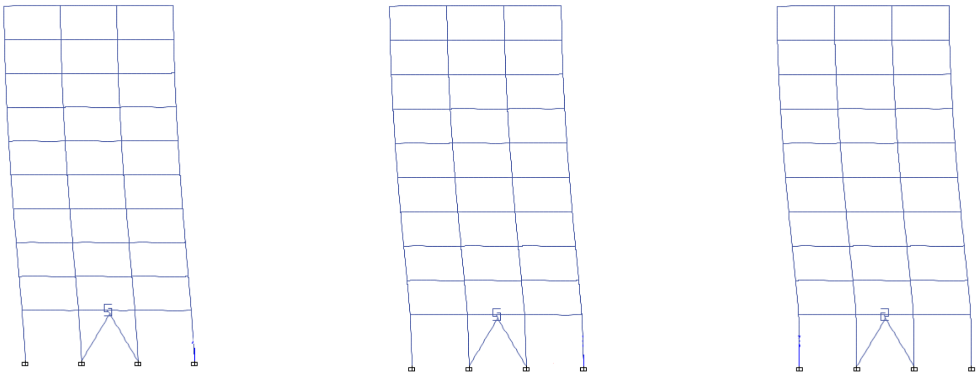

B10-4 ($T = 0.62\ s$) B10-5 ($T = 0.58\ s$) B10-6 ($T = 0.56\ s$)

Fig. 6. First mode shape of the ten-story configurations.

The general shape of the first mode of the fifteen-story configurations (B15), shown in Fig. 7, follows the same trend of the five- and ten-story configurations. The first mode shapes of all the configurations were nearly identical to the extent that the three vertical shear links in the configuration B15-3 did not noticeably affect the overall deformed shape of the configuration compared to the other configurations equipped with only single vertical shear link. Additionally, there was not much difference in the fundamental period (T) of the first mode shape between each configuration, as shown in the same figure. This appeared because of the placement of the vertical shear link in the first few stories of the building B15, thus, not contributing to the overall response of the building. The decrease in the fundamental period (T) of the first mode shape for the fifteen-story configurations compared to the original configuration ranged from 1 to 7% which was, for sure, less than the percentage of the decrement in the case of five- and ten-story configurations.

4.2. Nonlinear static pushover analysis

A nonlinear static pushover analysis is usually performed by exposing the superstructure to monotonically increasing lateral loads or displacements. These lateral loads/displacements simulate the inertial forces which would be experienced by the structure when subjected to seismic action. Many sources found in literature propose different lateral load patterns to be adopted in the pushover analysis, such as single load, parabolic load scheme, inverted triangle, etc. (Mohsenian et al., 2020). However, the technique employed here depended on subjecting the roof to a single monitored displacement. Different structural elements may yield under the effect of the incrementally increasing monitored displacement and, in addition, at each event, the structure may lose stiffness and strength continuously. Based on a pushover analysis, a nonlinear relation between base shear and roof displacement can be obtained which, in turn, can be converted into the so-called capacity spectrum in order for the building performance to be assessed.

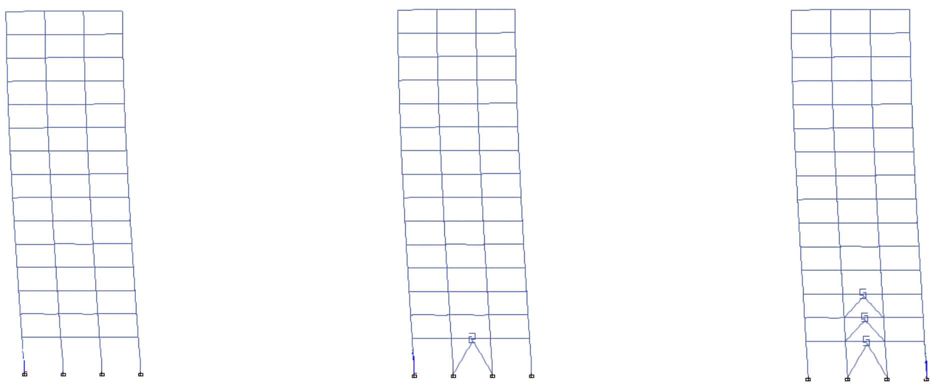

B15-1 ($T = 0.1\ s$) B15-2 ($T = 0.8\ s$) B15-3 ($T = 0.79\ s$)

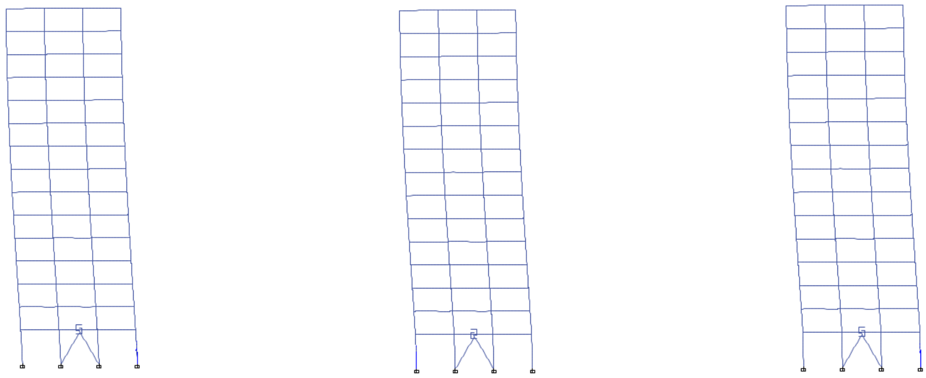

B15-4 ($T = 0.79\ s$) B15-5 ($T = 0.77\ s$) B15-6 ($T = 0.75\ s$)

Fig. 7. First mode shape of the fifteen-story configurations.

Fig. 8 shows a plot of the base shear and roof displacement for the five-story configurations. As noticed, the configurations containing vertical shear links, B5-2 to B5-6, had higher elastic lateral stiffness compared to the original bare configuration, B5-1. It is also clear that configurations B5-5 and B5-6 (containing steel vertical shear links) had higher ductility compared to the other configurations. Concerning the configurations attitude under the effect of lateral loads, it is assessed counting on determining the performance level at the performance point which was generally measured in terms of member rotations as per (ASCE/SEI 41, 2017). Although the performance level of the original bare building, B5-1, laid in the immediate occupancy (IO) level, installation of vertical shear links in the other configurations managed to shift their performance towards the operational region (O), therefore, having less roof drift, and upgraded performance (i.e., no permanent structural damage), as illustrated in Table 3. Nevertheless, the configuration B5-6 was the only one that failed to improve the seismic performance of the building B5 despite its capability to decrease the number of the plastic hinges lying in the IO stage. This remarks an important point since the configuration B5-6 was installed with the vertical shear links specimen 12 which had the highest yield force among all other specimens, and it also had the maximum amount of dissipated energy when subjected to cyclic loading; Refer to (El-Gammal et al., 2021; Seleemah et al., 2022) for more information.

The pushover curves, shown in Fig. 9, reveal that the ten-story configurations equipped with vertical shear links were characterized with large lateral stiffness and base shear carrying capacity compared to the original configuration, B10-1. Moreover, configurations B10-5 and B10-6 exhibited more ductility compared to the other configurations of the building B10. In spite of the configuration B10-3 being equipped with three vertical shear links of the specimen 25, no obvious increase in the base shear carrying capacity compared to the configuration B10-2, including single vertical shear link of the same specimen, is observed. Due to the increased number of stories in the current building, B10, compared to the previous building, B5, not all of the configurations managed to upgrade the performance level of the current building. It is neat in Table 4 that original configuration of the building laid in the life safety (LS) performance level while only configurations B10-3 and B10-5, installed with single magnesium and steel vertical shear link, respectively, shifted the performance level towards the O level. Therefore, it is demonstrated again that the optimum configurations were not those installed with large numbers of vertical shear links nor with the vertical shear link having the largest yield force; The optimum configurations were the ones having consistency between the base shear acting on the building and the characteristics of the equipped vertical shear link.

0 0.1 0.2 0.3 0.4

Roof displacement (m)

Fig. 8. Pushover curves for the five-story configurations.

Table 3. Details of the plastic hinges for the five-story configurations.

Configuration	A-B	B-IO	IO-LS	LS-CP	Beyond CP	Performance Level
B5-1	67	3	0	0	0	IO
B5-2	72	0	0	0	0	O
B5-3	76	0	0	0	0	O
B5-4	72	0	0	0	0	O
B5-5	72	0	0	0	0	O
B5-6	71	1	0	0	0	IO

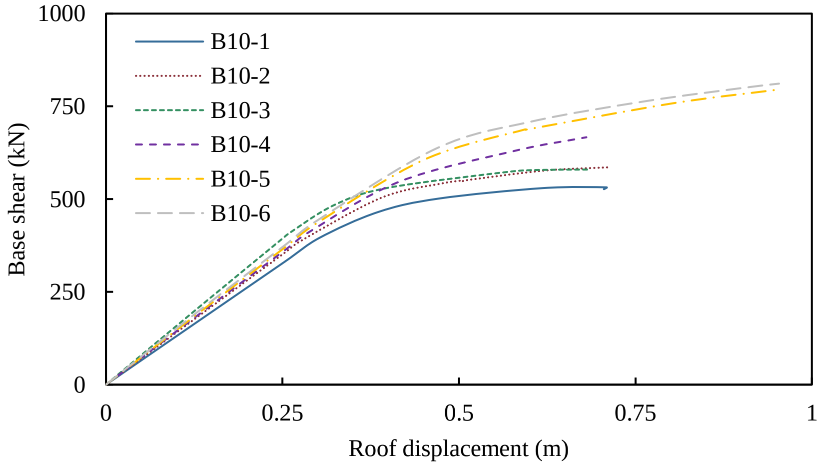

Fig. 9. Pushover curves for the ten-story configurations.

Table 4. Details of the plastic hinges for the ten-story configurations.

Configuration	A-B	B-IO	IO-LS	LS-CP	Beyond CP	Performance Level
B10-1	132	4	4	0	0	LS
B10-2	139	3	0	0	0	IO
B10-3	146	0	0	0	0	O
B10-4	141	1	0	0	0	IO
B10-5	142	0	0	0	0	O
B10-6	141	1	0	0	0	IO

As discussed before in the fundamental period (T) results of the fifteen-story building, B15, installation of vertical shear links only in the first few stories did not significantly alter the building behavior. The pushover curves, shown in Fig. 10, emphasize that observation since no obvious increase in the base shear of the configurations equipped with vertical shear links is found when compared to the original configuration, B15-1. However, in the current building, the configurations having relatively more ductility with respect to the others were B15-3 and B15-6 which were installed with three magnesium vertical shear links of the specimen 25 and a single steel vertical shear link of the specimen 12, respectively. The reason for these configurations to overpass the others in the fifteen-story building is that the building had more stories and increased weight which mark the need for a larger number of vertical shear links or having vertical shear links with large yield force and energy dissipation capacity. Regarding the performance level of the fifteen-story configurations, illustrated in Table 5, the original configuration had a performance level of LS. Additionally, all of the configurations, except B15-6, were not able to enhance the performance level of the building; B15-6 was the only configuration capable of changing the performance level to IO. The nearest competitor to that configuration was B15-3.

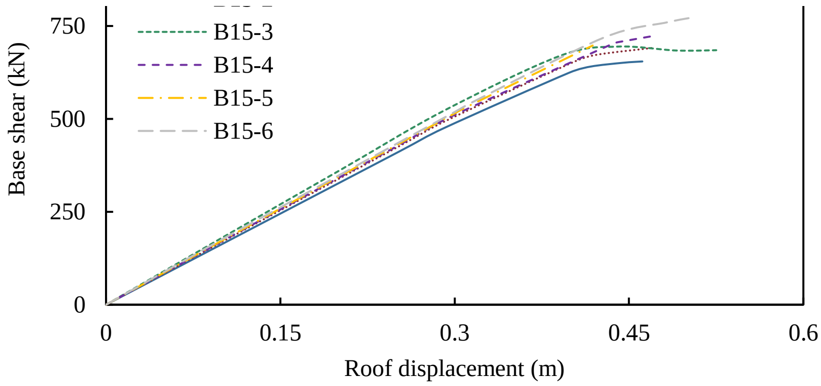

Fig. 10. Pushover curves for the fifteen-story configurations.

Table 5. Details of the plastic hinges for the fifteen-story configurations.

Configuration	A-B	B-IO	IO-LS	LS-CP	Beyond CP	Performance Level
B10-1	132	4	4	0	0	LS
B10-2	139	3	0	0	0	IO
B10-3	146	0	0	0	0	O
B10-4	141	1	0	0	0	IO
B10-5	142	0	0	0	0	O
B10-6	141	1	0	0	0	IO

4.3. Nonlinear dynamic time-history analysis

Nonlinear dynamic time history analysis is the most reliable and realistic technique to evaluate seismic behavior of structures, as it considers the properties of the structure as a whole in the analysis. This technique is also sophisticated, time consuming and highly sensitive to small changes in assumptions. In order to study the configurations response under real earthquake histories, component N45°E of 1979 Imperial Valley earthquake (Fig. 11) was chosen for the nonlinear time history analysis. This particular earthquake has a peak ground acceleration of nearly 0.32g.

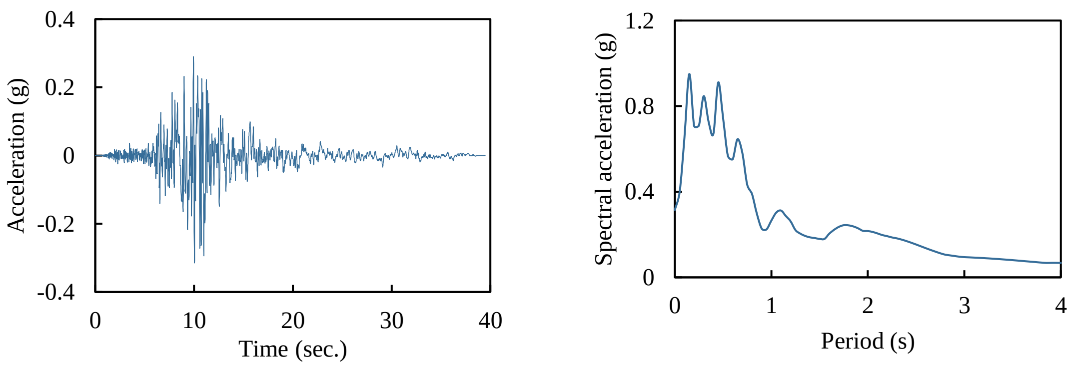

Fig. 11. Acceleration history and response spectrum of the Imperial Valley 1979 earthquake.

The first parameter to take into account when evaluating nonlinear time history analysis results for the five-story building is the maximum imposed base shear acting on the structure during the seismic event. To facilitate the comparison of the results, maximum base shear for each configuration, B5-2 to B5-6, was normalized through dividing it by the maximum base shear acting on the original configuration, B5-1, and plotted in Fig. 12. It is seen that the maximum base shear acting on the building during the earthquake was greatly affected by the installation of vertical shear links since the normalized base shear for each configuration was greater than unity. Generally speaking, increasing the stiffness of the building by vertical shear links should induce larger base shear. Yet, this is not always applicable since the applied earthquake has a response spectrum containing several ups and downs (not smooth envelope one). This interprets the case under study in which, for instance, B5-6 had lower base shear compared to B5-5 in spite of having slightly more lateral stiffness. As appearing in Fig. 13, installation of vertical shear links into the building did not much change the whole building deformed shape, however, it resulted into decreasing the story displacements in comparison with the original bare building, B5-1. Among all of the configurations equipped with vertical shear links, except B5-6, that were proved previously to upgrade the performance level of the five-story building, B5-5, was the configuration having the least story displacements. The maximum story displacement of B5-5 was about 38% of the same value of B5-1. With respect to the maximum interstory drifts of the five-story configurations in Fig. 13, it is found that the buildings installed with vertical shear links have relatively lower interstory drifts compared to the one without vertical shear links, B5-1. Putting the light on the more favorable configuration, B5-5, it is obvious that it had maximum interstory drift of 0.2% which represented about 37% of the maximum interstory drift of the original building, B5-1. As previously reported in literature, the main role of the vertical shear links in the building is to dissipate energy through inelastic deformations whereas the main structural elements are kept safe responding elastically. However, equipping the configurations with vertical shear links, having different parameters, resulted in the change of the earthquake input energy as well as the hysteretic energy in the system. Therefore, ratio of the dissipated hysteretic energy (EH) to the earthquake input energy (EI) is shown in Fig. 15. It is visible that the configuration B5-5 (containing vertical shear link specimen 11) was the one capable of dissipating the greatest ratio of input energy among all other configurations although specimen 11 was one step behind specimen 12 (equipped in B5-6) in terms of dissipating energy when subjected to cyclic loading. This supports the belief that dissipating large amount of energy under cyclic loading conditions does not necessary mean that the vertical shear link is capable of dissipating the same amount of energy during earthquake event. The reason is that vertical shear links exposed to cyclic loading are forced to displace in certain directions with specific displacements while this is not the case when earthquake takes place since story displacements are mainly dependent on the characteristics of the building and the lateral load resisting system (e.g., stiffness, fundamental period, etc.). Another factor to be considered is the time delay of the vertical shear link operation which can be defined as the time required for the vertical shear link to yield and start dissipating energy (i.e., EH>0). As shown in Fig. 14, configuration B5-5 again had the lowest time delay of 2.42 s. so it is predicted to yield quickly compared to other proposed configurations.

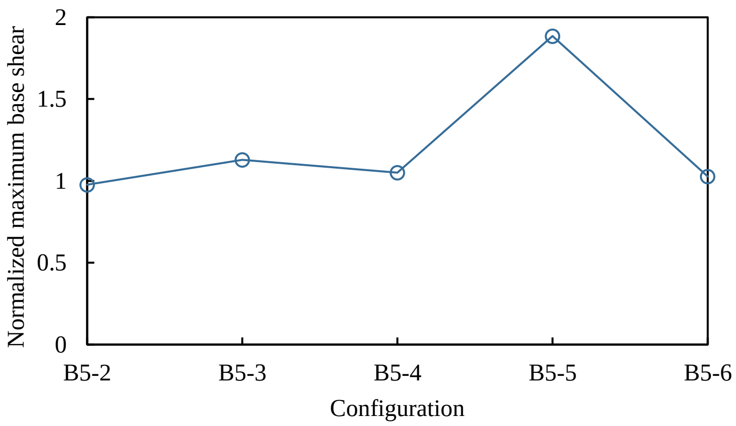

Fig. 12. Normalized maximum base shear for the five-story configurations.

Fig. 13. Maximum story displacements and interstory drifts of the five-story building configurations.

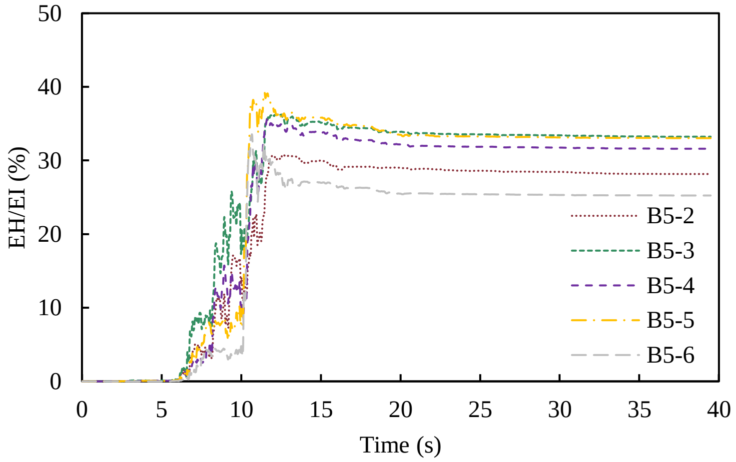

Fig. 14. Ratio of dissipated energy to earthquake input energy for the five-story building configurations.

Similar to what has been done earlier in the five-story configurations, the maximum base shear of the configurations B10-2 to B10-6 were normalized through dividing it by the maximum base shear of the original configuration, B10-1, as shown in Fig. 15. Normalized maximum base shear of the ten-story configurations depicted that all of the configurations equipped with vertical shear links had larger maximum base shear with respect to the original configuration, B10-1. The configurations which managed to upgrade the performance level of the ten-story building in the pushover analysis, B10-3 and B10-5, had increased base shear of 4 and 67%, respectively, compared to B10-1. More attention should be directed towards the global response, shown in Fig. 16, of the configurations B10-3 and B10-5. These two configurations had maximum story displacements of 79 and 64%, respectively, of that of the original bare building, B10-1. For the maximum interstory drifts of the buildings (Fig. 16), again, the configurations installed with vertical shear links had lower interstory drifts compared to the one without vertical shear links, B10-1. Moreover, the more favorable configurations, B10-3 and B10-5, had maximum interstory drifts of about 85 and 71% of the maximum interstory drift of the original building, B10-1, respectively. According to Fig. 20, The time delay for the optimum configurations of the ten-story building (i.e., B10-3 and B10-5) was found to be 3.75 and 2.95 s, respectively. This demonstrates the advantage of configuration B10-5 over B10-3. It is additionally obvious in Fig. 17 that B5-5 dissipated the largest amount of the earthquake input energy, nearly 29%. The other configuration which also upgraded the performance level of the ten-story building, B5-3, dissipated only 16% of the input energy.

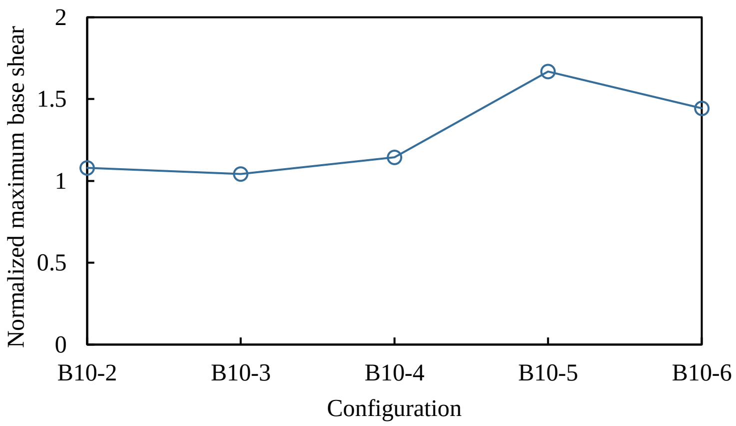

Fig. 15. Normalized maximum base shear for the ten-story configurations.

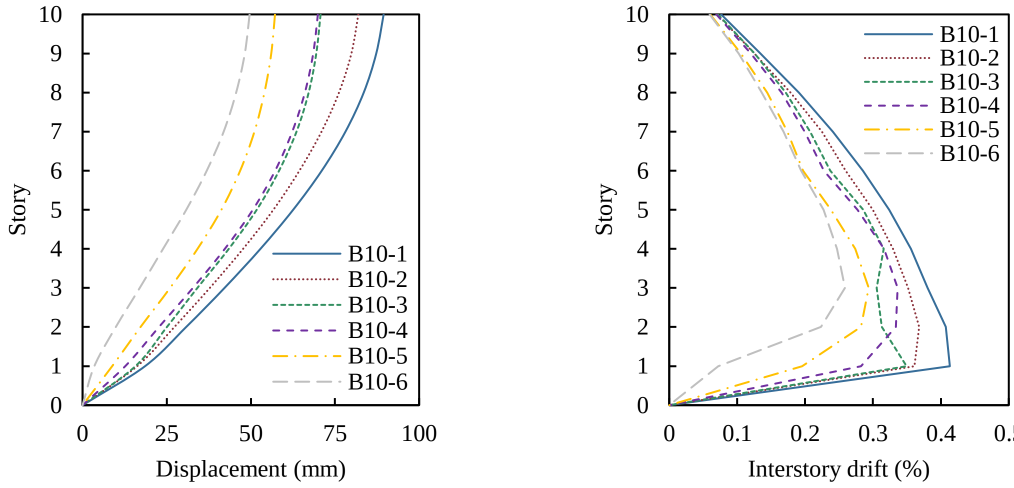

Fig. 16. Maximum story displacements and interstory drifts of the ten-story building configurations.

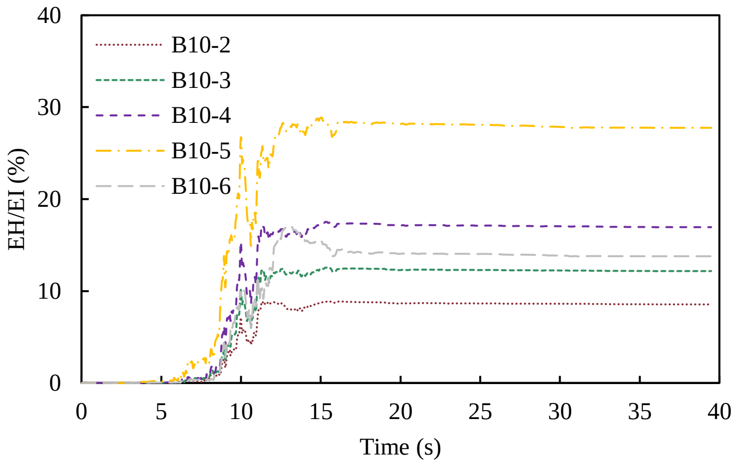

Fig. 17. Ratio of dissipated energy to earthquake input energy for the ten-story building configurations.

Maximum base shear for each fifteen-story configuration equipped with vertical shear links was normalized through dividing it by the maximum base shear of the original configuration, B15-1, and plotted in Fig. 18. All of the configurations equipped with vertical shear links had normalized values larger than unity especially the last two configurations, B15-5 and B15-6, which had normalized values of 1.34 and 1.51, respectively. This indicates an increase in the base shear acting on these configurations by nearly one-third to one-half. As previously discussed in the results of the pushover analysis, the only configuration that showed slight improvement in the performance level of the fifteen-story building was B15-6. This particular configuration had the lowest story displacements compared to the other configurations, as shown in Fig. 19. Its maximum story displacement represented about 85% of that of B15-1. Nonetheless, only using vertical shear links in the first few stories of B15 was not efficient in reducing story displacements. Also, configuration B15-6 managed to decrease the maximum interstory drift by about 12% only compared to B15-1, as shown in the same figure. This is an indicative of the poor performance of the fifteen-story building equipped with vertical shear links in its first story only. Poor performance of all of the configurations of the fifteen-story building also represented in the fact that the highest ratio of dissipated energy took place in B15-6 and it represented only 19% of the input energy, as shown in Fig. 20. The remaining input energy, not absorbed by the vertical shear link, was directed towards the main structural elements of the building causing it to have poor performance level. Configuration B15-6 had a time delay of 4.49 s. which is considered large. This means that for the first 12% of the seismic event duration, the main structural elements were responsible alone for carrying earthquake loads and dissipating the input energy. Configuration B15-5, which dissipated only 15% of the input energy, had the lowest time delay of 3.63 s.

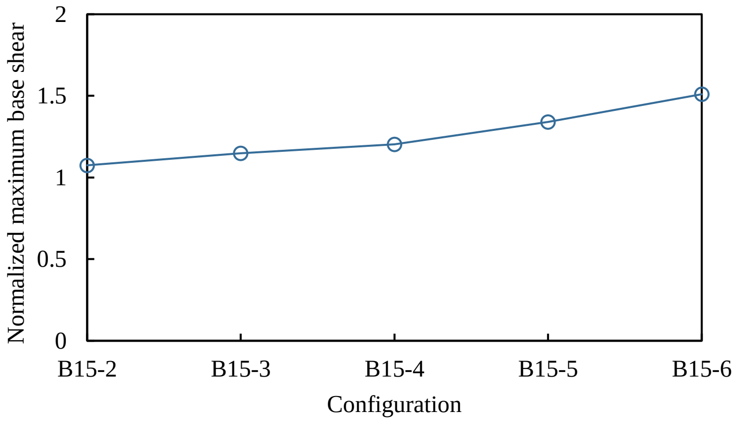

Fig. 18. Normalized maximum base shear for the fifteen-story configurations.

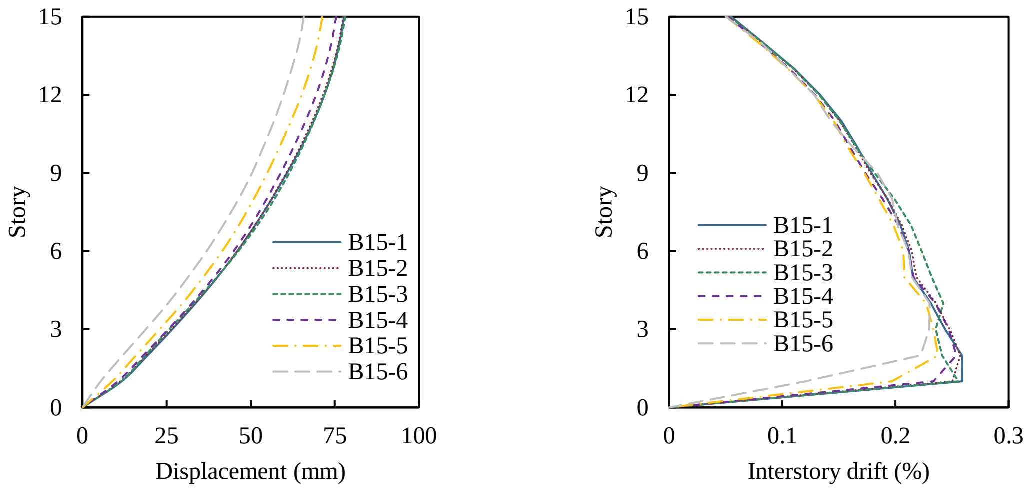

Fig. 19. Maximum story displacements and interstory drifts of the fifteen-story building configurations.

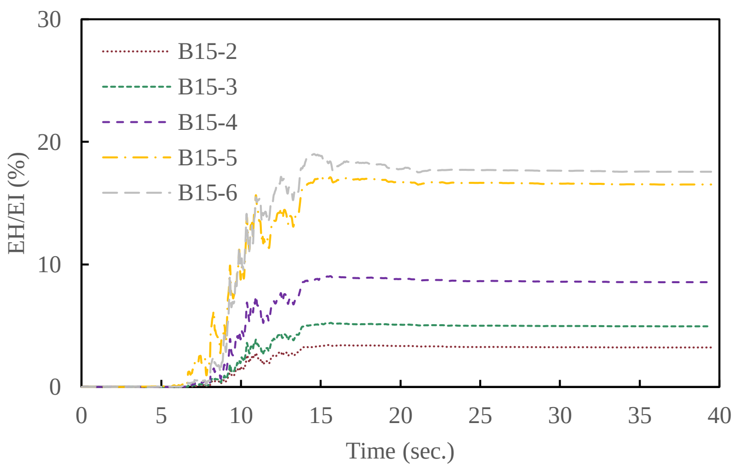

Fig. 20. Ratio of dissipated energy to earthquake input energy for the fifteen-story building configurations.

5. Conclusions

A numerical investigation was conducted on steel moment-resisting frames, using the finite element software ETABS (18.0.0) (Computers and Structures, 2018), to evaluate their seismic response in their original bare condition and in the case of strengthening them with eccentric braces and one of the yielding metallic dampers known as “vertical shear links” in certain bays; thus, transforming them into eccentrically braced frames. The buildings number of stories ranged from five to fifteen. Two magnesium and two steel vertical shear links, previously analyzed in an earlier study of the authors, were selected to be installed into the buildings yielding eighteen different configurations. Relying on the results of the modal analysis, nonlinear static pushover analysis and the nonlinear time history analysis, the following concluding remarks could be drawn out:

(a) Installation of vertical shear links in 2-D moment-resisting frame resulted in a change in their lateral stiffness and thus a change in their first mode fundamental period. In fact, all buildings equipped with vertical shear links had their fundamental period shortened compared to the original deficient buildings.
(b) Pushover analysis results indicated that installing vertical shear links into certain bays of the buildings upgraded their performance level. However, no great improvement was observed for the fifteen-story building.
(c) Time-history analysis results showed that the five- and ten-story buildings installed with vertical shear links had lower story displacements and interstory drifts in comparison with the original building. In the fifteen-story building, minor decrease in the story displacements and interstory drifts was observed when equipping them with vertical shear links.
(d) For the studied low- to mid-rise buildings, vertical shear links can be installed in the first few stories only while producing acceptable seismic response. On the contrary, installation of vertical shear links on the first few stories of the fifteen-story building was not sufficient and barely had influence on the seismic response.
(e) A vertical shear link dissipating large amount of energy under cyclic loading conditions does not necessary mean that the same vertical shear link is capable of dissipating similar amount of energy during earthquake event. For instance, for most of the studied configurations, the steel vertical shear link (having moderate strength and stiffness) performed better than the stiffer steel vertical shear link in dissipating seismic energy and enhancing the seismic response of the buildings.

Disclosure
The authors report no conflicts of interest in this work.

References

American Institute of Steel Construction (AISC). Specifications for structural steel buildings: ANSI/AISC 360-16. Chicago, USA. 2016.

American Society of Civil Engineers (ASCE). Seismic evaluation and retrofit of existing buildings: ASCE/SEI 41-17. Reston, USA. 2017.

Baradaran M, et al. The effect of vertical shear-link in improving the seismic performance of structures with eccentrically bracing systems. International Journal of Civil and Environmental Engineering. 2015; 9(8): 1086-1090.

Bouwkamp J, Vetr M, Ghamari A. An analytical model for inelastic cyclic response of eccentrically braced frame with vertical shear link (V-EBF). Case Studies in Structural Engineering. 2016; 6: 31-44.

Bozkurt M, Topkaya C. Replaceable links with gusseted brace joints for eccentrically braced frames. Soil Dynamics and Earthquake Engineering. 2018; 115: 305-318.

Chacón R, Vega A, Mirambell E. Numerical study on stainless steel I-shaped links on eccentrically braced frames. Journal of Constructional Steel Research. 2019; 159: 67-80.

Chesoan A, Stratan A, Dubina D. Design implementation of re-centring dual eccentrically braced frames with removable links. Soil Dynamics and Earthquake Engineering. 2018; 112: 174-184.

Computers and Structures Inc. ETABS (18.1.1). Walnut Creek, USA. 2018.

Daryan A, et al. Seismic behavior of vertical shear links made of easy-going steel. American Journal of Engineering and Applied Sciences. 2008; 1(4).

De Matteis G, Mistakidis E. Seismic retrofitting of moment resisting frames using low yield steel panels as shear walls. In: Stessa 2003. Routledge. 2018; 677-682.

Di Sarno L, Elnashai A. Bracing systems for seismic retrofitting of steel frames. Journal of Constructional Steel Research. 2009; 65(2): 452-465.

Duan L, Su M. Seismic testing of high-strength steel eccentrically braced frames with a vertical link. Proceedings of the Institution of Civil Engineers-Structures and Buildings. 2017; 170(11): 874-882.

Durucan C; Dicleli M. Analytical study on seismic retrofitting of reinforced concrete buildings using steel braces with shear link. Engineering Structures. 2010; 32(10): 2995-3010.

Elgammal A. Improving the performance of vertical shear links for enhanced seismic energy dissipations. M.Sc. Thesis, Tanta University. Tanta, Egypt. 2021.

Elgammal A, Seleemah A. Near-field earthquake performance of eccentrically braced steel buildings with supplemental fluid viscous dampers. Proceedings of the International Conference on Advances in Structural and Geotechnical Engineering. Hurghada, Egypt. 2023.

El-Gammal A, El-Khoriby S, Seleemah A. Seismic response of 2-D plane framed buildings eccentrically braced with vertical shear links. Proceedings of the International Conference on Advances in Structural and Geotechnical Engineering. Hurghada, Egypt. 2021.

Ghadami A, et al. Overstrength factor of short low-yield-point steel shear links. Thin-Walled Structures. 2021; 161: 107473.

Li T, et al. Real-time hybrid simulation on high strength steel frame with Y-shaped eccentric braces. Engineering Structures. 2021; 226: 111369.

Lignos D, et al. Comparison of retrofitting techniques for existing steel moment resisting frames. Improving the Seismic Performance of Existing Buildings and Other Structures. 2010; 988-999.

Maniyar S; Paul D. Enhancement of seismic performance using shear link Braces in a building designed only for gravity loads. Journal of The Institution of Engineers. 2012; 93: 27-43.

Mansour N, Christopoulos C, Tremblay R. Experimental validation of replaceable shear links for eccentrically braced steel frames. Journal of Structural Engineering. 2011; 137(10): 1141-1152.

Mazzolani F, Corte G, D'Aniello M. Experimental analysis of steel dissipative bracing systems for seismic upgrading. Journal of Civil Engineering and Management. 2009; 15(1): 7-19.

Mirzai N, Attarnejad R. Seismic performance of EBFs equipped with an innovative shape memory alloy damper. Scientia Iranica. 2020; 27(5): 2316-2325.

Mohsenian V, Mortezaei A. A new energy-absorbing system for seismic retrofitting of frame structures with slender braces. Bulletin of Earthquake Engineering. 2019; 17(5): 2715-2739.

Mohsenian V, Nikkhoo A. Evaluation of performance and seismic parameters of eccentrically braced frames equipped with dual vertical links. Structural Engineering and Mechanics. 2019; 69(6): 591-605.

Mohsenian V, et al. Seismic performance evaluation of deficient steel moment-resisting frames retrofitted by vertical link elements. Structures. 2020; 26: 724-736.

Mohsenian V, Hajirasouliha I, Filizadeh R. Seismic reliability analysis of steel moment-resisting frames retrofitted by vertical link elements using combined series–parallel system approach. Bulletin of earthquake engineering. 2021; 19(2): 831-862.

Rai D, Annam P, Pradhan T. Seismic testing of steel braced frames with aluminum shear yielding dampers. Engineering Structures. 2013; 46: 737-747.

Rajeswaran G, Wijeyewickrema A. An alternative design method for the seismic retrofit of RC moment resisting frame buildings with viscous dampers. Journal of Earthquake Engineering. 2022; 26(1): 240-270.

Rahnavard R, et al. Evaluation on eccentrically braced frame with single and double shear panels. Journal of Building Engineering. 2017; 10: 13-25.

Seleemah A, El-Khoriby S, El-Gammal A. Seismic response of 2-D plane framed buildings eccentrically braced with vertical shear links. International Journal on Advances in Structural and Geotechnical Engineering. 2021; 5(4): 1-18.

Shu Z, et al. Experimental and numerical investigations of replaceable moment-resisting viscoelastic damper for steel frames. Journal of Constructional Steel Research. 2020; 170: 106100.

Seki M, et al. Study on earthquake response of two-storied steel frame with Y-shaped braces. Proceedings of the 9th world conference on earthquake engineering. Tokyo-Kyoto, Japan. 1988.

Tafsirojjaman T, Fawzia S, Thambiratnam D. Numerical investigation on the seismic strengthening of steel frame by using normal and high modulus CFRP. Proceedings of the 7th Asia Pacific Conference on FRP in Structures. Brisbane, Australia. 2019.

TahamouliRoudsari M, et al. Experimental assessment of retrofitting RC moment resisting frames with ADAS and TADAS yielding dampers. Structures. 2018; 14: 75-87.

Vetr M, Ghamari A, Bouwkamp J. Investigating the nonlinear behavior of Eccentrically Braced Frame with vertical shear links (V-EBF). Journal of Building Engineering. 2017; 10: 47-59.

Wen Y. Method for random vibration of hysteretic systems. Journal of the engineering mechanics division. 1976; 102(2): 249-263.

Zahrai M, Mahroozadeh Y. Experimental study of using vertical link beam to improve seismic performance of steel buildings. Journal of Civil and Surveying Engineering. 2010; 44(3).

Zhu Y, et al. Finite element modeling and design recommendations for low-yield-point steel shear panel dampers. Journal of Building Engineering. 2023; 72: 106634.